This full text paper was peer-reviewed at the direction of IEEE Instrumentation and Measurement Society prior to the acceptance and publication.

Multi-Gaussian Model for Estimating Stiffness Surrogate using Arterial Diameter Waveform

Rahul Manoj
Department of Electrical Engineering
Indian Institute of Technology Madras
Chennai, India
rahul_manoj@smail.iitm.ac.in

Raj Kiran V
Department of Electrical Engineering
Indian Institute of Technology Madras
Chennai, India
ee15d020@smail.iitm.ac.in

Nabeel PM
Healthcare Technology Innovation Centre (HTIC), IIT Madras
Chennai, India
nabeel@htic.iitm.ac.in

Mohanasankar Sivaprakasam
Department of Electrical Engineering
Indian Institute of Technology Madras
Chennai, India
mohan@ee.iitm.ac.in

Jayaraj Joseph
Department of Electrical Engineering
Indian Institute of Technology Madras
Chennai, India
jayaraj@ee.iitm.ac.in

2021 IEEE International Symposium on Medical Measurements and Applications (MeMeA) | 978-1-6654-1914-7/20/$31.00 ©2021 IEEE | DOI: 10.1109/MeMeA52024.2021.9478600

***Abstract*— Central Arteries' elastic nature plays a fundamental role in maintaining cardiovascular health. Timely assessment of arterial stiffness helps in cardiovascular risk stratification. Various technological and methodological approaches exist to estimate arterial stiffness, through direct measurement of stiffness markers or surrogates. This work highlights a potential surrogate for arterial stiffness, based on the early onset of reflection waves. The significance comes with using low frame rate A-mode ultrasound scans for processing arterial diameter, modelled as a sum of three Gaussians. The novelty lies in the Gaussian modelled reflection onset time (τ_R^{GM}), derived using the model parameters, a potential surrogate for early reflections and arterial stiffness. An observational cross-sectional study group of 34 subjects were recruited to validate this hypothesis. A statistically significant ($p < 0.0001$) correlation was obtained for τ_R^{GM} against known stiffness markers. An $R > 0.85$ was obtained against Elastic modulus, specific stiffness index, and Pulse wave velocity. There exists an inverse correlation between the τ_R^{GM} and popular stiffness markers. A statistically significant ($p < 0.0001$) correlation was obtained for τ_R^{GM} against age, with $R = 0.56$. The early reflections were reliably detected by the τ_R^{GM} and the evidenced strong correlation with stiffness markers make it a potential surrogate for arterial stiffness assessment. The advantage being that it can be obtained from a single pulse waveform like diameter.**

Keywords—Gaussian model, early reflection, arterial stiffness, pulse wave velocity, vascular ageing, ultrasound, diameter, carotid, Levenberg-Marquardt, optimisation

I. Introduction

The elastic nature of central arteries plays a vital role in pulsatile haemodynamics of the circulatory system, by storing the pulsatile energy from intermittent ventricular ejection. This helps maintain a steady flow in microcirculation by dampening the pulsatile nature of blood flow along the arterial tree for efficient tissue perfusion [1]. In clinical practice, arterial stiffness is the measure of compliance of conduit arteries.

The clinically popular functional stiffness metrics are derived from direct measurement of pressure and arterial geometry, namely volume Elastic modulus (or Peterson elastic modulus E_P), Arterial Compliance (AC) and specific stiffness index (β), shown in TABLE I. For the non-invasive measurement of arterial geometric properties ultrasound imaging is employed, and this makes it difficult to simultaneously acquire pressure measurements from the same site, owing to the large form factor of the imaging probes [2]. Additionally, measurement of these stiffness metrics from central arteries is even more challenging due to the lack of a reliable central blood pressure measuring device [3].

Pulse wave velocity (PWV), a surrogate measure of arterial elasticity, have gained clinical attention due to the easier methodological advantage [4]. The PWV derived from pulse propagation time measured between a blood pulse waveform and R-Peak of ECG [5], suffers bias due to the cardiac pre-ejection period. Therefore, more reliable methods are based on estimating the pulse propagation times from identical blood pulse signals recorded from multiple arterial target sites [6]–[9]. There are also other methods where PWV evaluation requires capturing two distinct physiological signals from a single arterial site [10]. Nevertheless, these methods still require unimodal or multimodal instrumentation involving acquisition from multiple sites.

Contrary to the above-alluded methods, the pulse contour analysis technique involves the estimation of a stiffness surrogate from a single pulse waveform. One of the major measures includes the augmentation index (AIx), a qualitative representation of arterial reflection. The arterial tree's complex nature comprising diameter changes, bifurcations, and elasticity gradient introduces pulse waves reflection. The reflections further represent elasticity changes because of ageing. As the central arteries become stiffer, they cause faster propagation of backward waves leading to early reflections in the pulse wave. Hence parameters related to arterial wave reflections have also gained attention as potential stiffness surrogates. Though, AIx is the prevalent method in pulse counter analysis (PCA) that quantifies the amount of reflection in a pulse wave, it has several limitations as reported in [11].

In this work, we present a method to quantify a surrogate marker of stiffness evaluated from diameter waveform alone. This stiffness marker represents the onset of early blood pulse reflections. The proposed method models the recorded arterial diameter waveform using a multi-Gaussian approach and evaluates the early reflections' onset time based on the model parameters. Our clinically validated image-free ultrasound device, ARTSENS® [12], was used to record the

978-1-6654-1914-7/21/$31.00 ©2021 IEEE

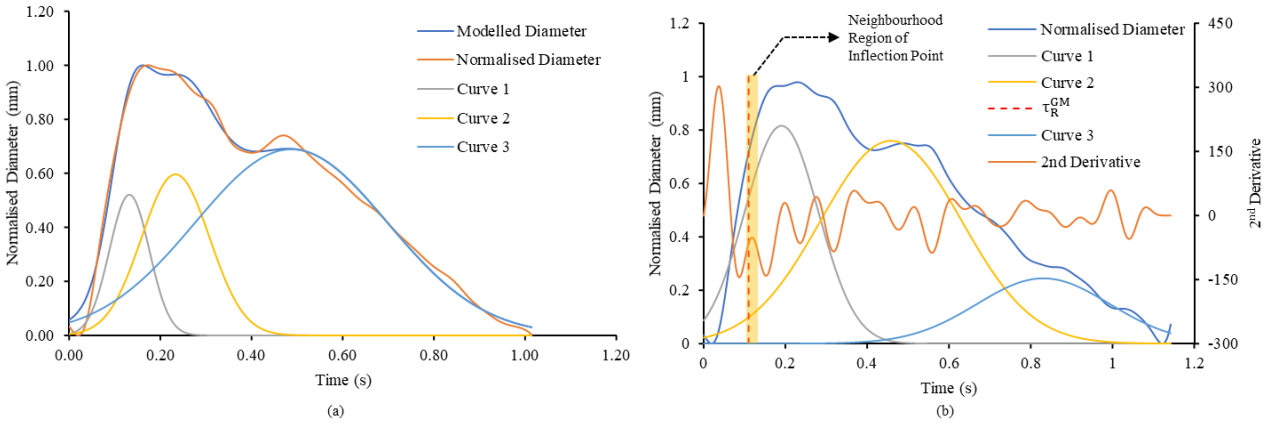

Figure 1. (a) Modelling of arterial diameter as sum of three Gaussians, (b) Point of inflection from high frame rate second derivative waveform and the Gaussian modelled reflection onset time.

arterial diameter waveforms. The proposed modelling approach and its implementation are presented in the subsequent section. The details on data collection with ARTSENS® device [12] and the conducted in-vivo validation study are presented in section III. Results are presented and discussed in section IV followed by the study limitations and conclusion.

II. Principle of Measurement

A. Multi-Gaussian Model of Arterial Distension Wave

A normalised arterial pulse waveform can be represented by a sum of Gaussian curves model [13]. In this work, we have approached modelling of the diameter waveform as the sum of three Gaussian curves. The sum of these three Gaussian curves with their respective amplitudes (A_i, i= 1, 2, 3), Gaussian mean locations (M_i, i= 1, 2, 3) and standard deviation locations from respective means (C_i, i = 1, 2, 3) on the time axis is expressed in (1).

$$D_M(P, t) = \sum_{i=1}^{3} A_i \, e^{-\frac{1}{2}\times\frac{(t-M_i)^2}{C_i^2}} \qquad (1)$$

Where $D_M(t)$ is the modelled diameter waveform, P is the Gaussian parameter set consisting of nine variables {Ai, Mi, Ci, i = 1, 2, 3} and t the time axis. This non-linear Gaussian model is fit to the normalised diameter waveform cycles. For robust curve fitting Levenberg-Marquardt (LM) algorithm is applied, with P as the set of parameters to be optimised. The LM method, also known as the damped least-squares method, is used to solve non-linear least square curve fitting problems. The model has nine variables; hence, there are nine optimising parameters subjected to constrain: $0 < M_1 < M_2 < M_3 < CW$; CW is the width of the pulse cycle.

Using LM method, for a given set of empirical data pair points of the independent and dependent variable, that is (t, D(t)), where D(t) is the acquired diameter waveform for a single cardiac cycle; the optimising problem is to find the parameter P = {A_i, M_i, C_i, i = 1, 2, 3} of the model curve $D_M(t)$, in such a way that the sum of least squares of the deviations S(P) is minimised:

$$\hat{P} \in \operatorname{argmin}_P S(P) \equiv \operatorname{argmin}_P \sum_{i=1}^{m} \left[D(t_i) - D_M(P, t_i)\right]^2 \qquad (2)$$

TABLE I Stiffness Markers

Stiffness Marker	Expression
Elastic modulus (Peterson) (kPa)	$E_P = \frac{\Delta P}{\Delta D/D}$
Specific Stiffness, β	$\beta = \frac{\ln(\frac{P_S}{P_D})}{\Delta D/D}$
PWV (From Bramwell-Hill Equation)	$PWV = \sqrt{\frac{D_D}{2\rho}\times\frac{\Delta P}{\Delta D}}$

The maximum number of iterations is set to 1000 and error tolerance of 1E-08. Cycles for which the optimisation crosses 1000 iterations or falls below the error tolerance are rejected. The model is illustrated in Fig.1(a). The number of Gaussians is a trade-off between minimising the curve fit error and computational complexity. Three is the experimentally found required number of Gaussians to keep the curve fit error within the tolerance (sum of least square error < 1) and be fast enough for computation. Three Gaussian model is also adopted, as it represents a physiologically rational model for an arterial pulse, composing of a forward component, tidal component and a dicrotic component.

B. Model-Based Estimation of Early Reflection Waves' Onset Time

It is a common assumption that the early systolic phase is free from the influence of reflections[11]. This assumption has been countered to be untrue. The influence of early reflections is rather not evident due to the low bandwidth of the pulse signals that are acquired using low frame rate acquisition systems. Studies point out that, early reflection wave arrival time is observed as systolic foot inflection point on the second derivative waveforms of pulse wave (local maxima just after the first peak of 2nd derivative waveform), and is measurable when signals are acquired at higher bandwidth – higher frame rates with sufficient resolution [14], as illustrated in Fig.1(b).

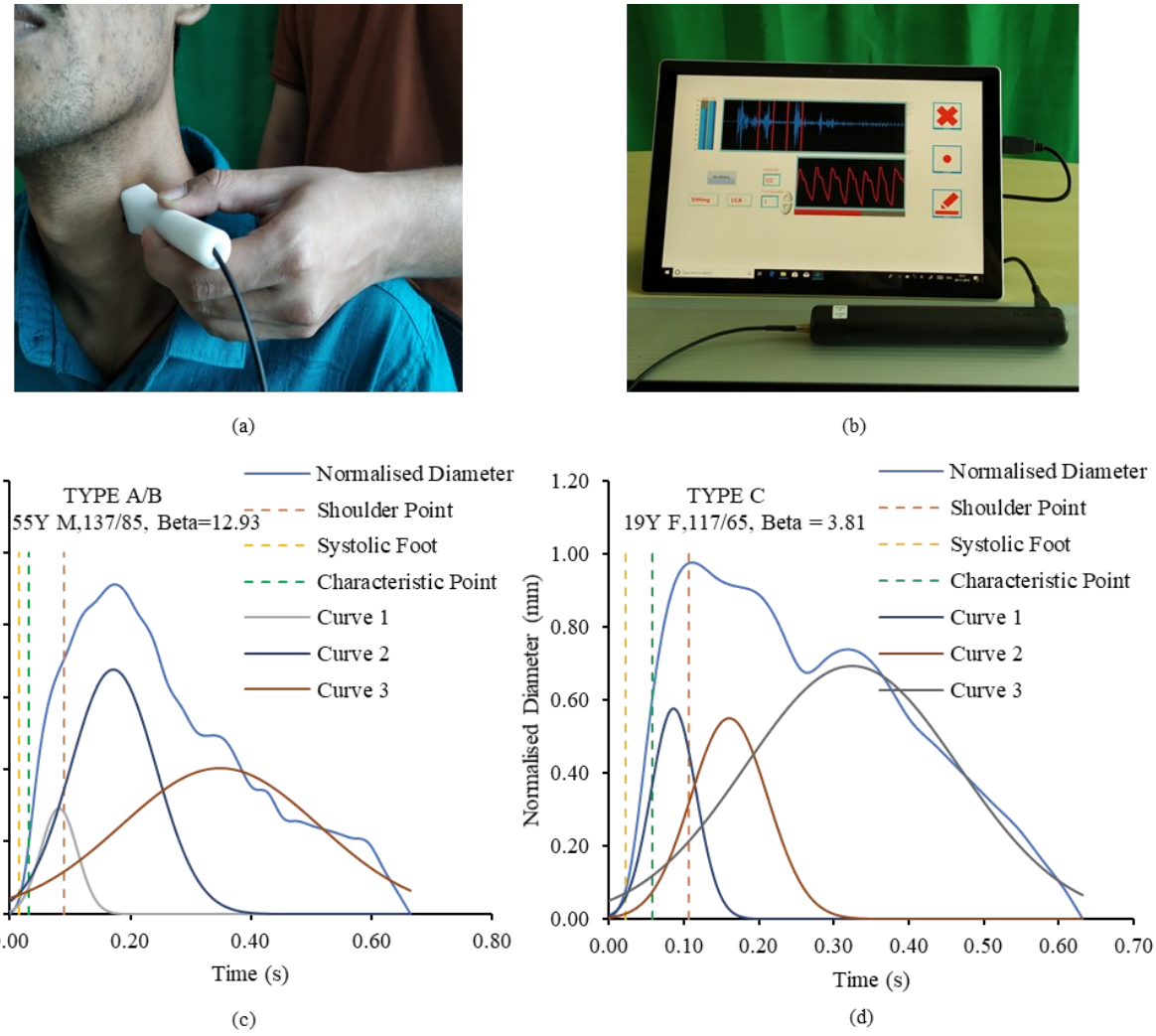

Figure 2. (a) ARTSENS® probe positioning on carotid artery, (b) Windows tablet running ARTSENS® software, (c) Type-A or Type-B waveform and its corresponding Gaussian curves, (d) Type-C waveform and its corresponding Gaussian curves.

A Gaussian modelled reflection onset fiducial point (φ_R^{GM}) was derived in this work from optimisation parameter set P, that resides in the immediate neighbourhood of the systolic foot inflection point, as highlighted in Fig.1(b). τ_R^{GM} is the Gaussian modelled reflection onset time, defined as the time difference between φ_R^{GM} and φ_{ED} .

$$\tau_R^{GM} = \varphi_R^{GM} - \varphi_{ED} \tag{3}$$

Where, φ_{ED} is the end-diastolic point and. This point (φ_R^{GM}) derived from the multi-Gaussian modelling, precisely represents the onset of early reflection wave. φ_R^{GM} was derived from model parameters M_2 and C_2 and is expressed as in (4),

$$\varphi_R^{GM} = M_2 - 2C_2 \tag{4}$$

Mathematically, (4) corresponds to 2σ (95% of data are within this region in a Gaussian curve) point of the second Gaussian curve in the sum of three Gaussian model. Since, the cycles are cut at end diastolic points, the origin of each cycle coincides with the end diastole, and we have,

TABLE II SUBJECT DEMOGRAPHY

Total Subjects	34
Male	18
Female	16
Age	18 – 71
Normotensive subjects	23
Hypertensive subjects	11
Type A/B waveform	28
Type C waveform	6
Systolic blood pressure (mmHg)	94 – 196
Diastolic blood pressure (mmHg)	56 – 100
Beta	2.2 – 13.4
Elastic modulus (kPa)	28.9 – 233.5
PWV (m/s)	3.42 – 9.14

$$\tau_R^{GM} = \varphi_R^{GM} \tag{5}$$

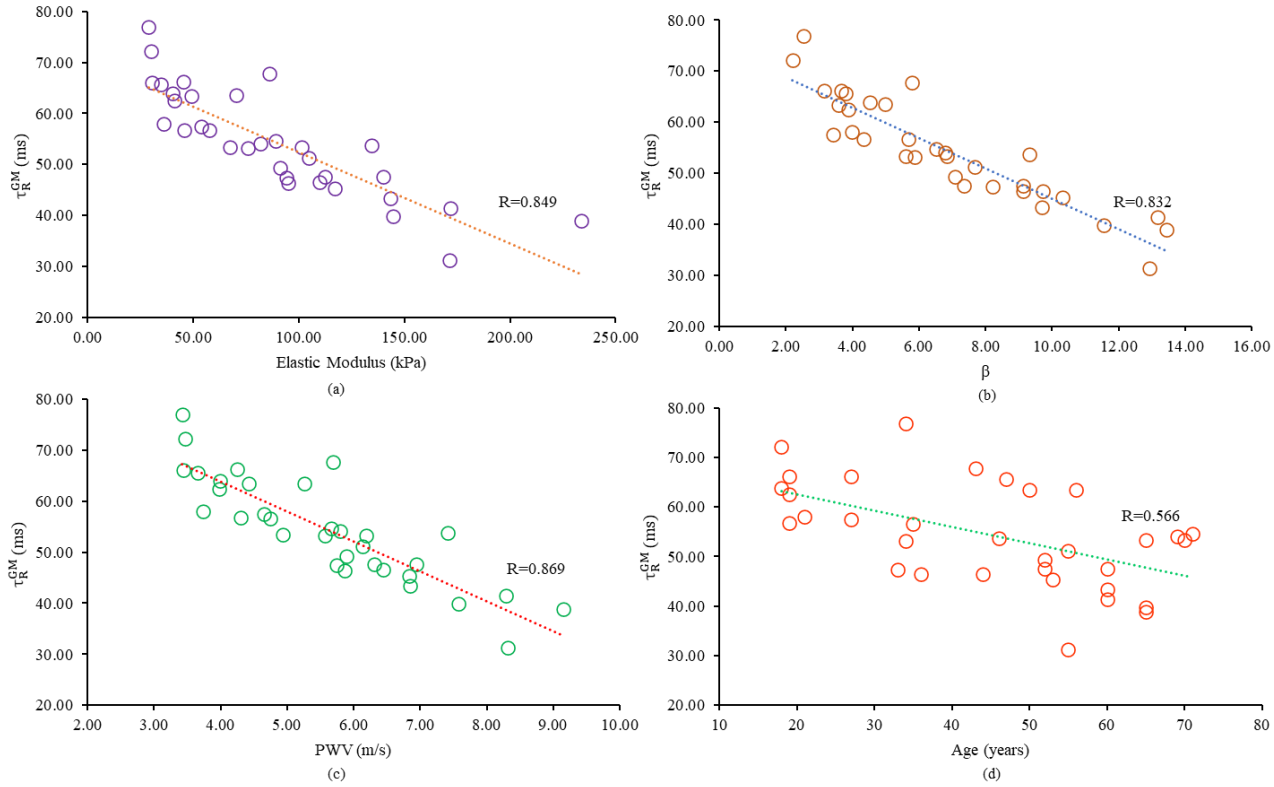

Figure 3. (a), (b), (c) Correlation with Stiffness markers, (d) Correlation with age

III. In-Vivo Validation Study

A. Study Selection

An observational cross-sectional study on thirty-four subjects (18 male and 16 female) was conducted at a multi-specialty hospital & research institute in Chennai, India. The study protocols were reviewed and approved by the Institutional Review Board (VHS-IEC/17-2016). A brief questionnaire was filled by the subjects describing their age, gender, physical activity level, diet habits and medications. Basic body measurements, like height and weight, were also obtained. They were familiarised with the procedure, devices used and testing environment, which will minimise the influence of anxiety, and the participants will be fully aware of the intentions of the experiment. Written consent for each subject is obtained in accordance with the World Medical Association Declaration of Helsinki: Ethical principles for medical research involving human subjects, revised in 2013. Two trials were performed for all participants.

B. Instrumentation & Measurement Protocol

All subjects were relaxed for 5-10 minutes before the measurement. Brachial BP was obtained using an automated BP monitor (SunTech®) on the left arm prior to the ultrasound measurement. Diameter and stiffness measurements were obtained by ARTSENS® [12]. The device consists of a single channel A-mode ultrasound transducer probe, associated software, and hardware for arterial stiffness evaluation. The ultrasound transducer is a 5 MHz, (diameter: 5 mm, spatial angle < 1.3◦) in an ergonomic probe. The transducer functions in pulse-echo mode at a depth of 40 mm, at frame rates of 40 Hz. The radio frequency (RF) echoes were sampled at 80 MHz by a 12-bit ADC. The digital controls to pulsar unit (STHV748) were controlled by a 32-bit ARM cortex M4 (LPC4370FET256, NXP Semiconductors) embedded with power supply and USB connection to a tablet running on Windows 10. The ARTSENS® measurement procedure involved locating the left carotid artery below the carotid bulb through palpation, followed by orienting the ARTSENS® pen probe to obtain sharp RF echoes moving in opposite sides corresponding to the walls of the artery. The transducer probe was held positioned for a sufficient number of cycles to complete the required stiffness parameters' measurement and processing.

The digitised RF echoes were processed in a LabVIEW based application. The frames were pre-processed using a 4th order bandpass zero-phase filters (Low cut off: 1 MHz, High cut off: 8 MHz). A time-varying gain was applied to compensate signal attenuation due to tissue layers (attenuation coefficient assumed to be 0.7dB/cm/MHz). The out of phase motion of the artery walls were exploited in developing the algorithm for detecting and tracking arterial walls. A sliding covariance window-based method was used for detecting the walls, and identified walls were continuously tracked by correlation-based techniques. Intelligent algorithms of ARTSENS® ensured RF echoes were captured at the high signal quality. Cycle-to-cycle distension and lumen diameter was estimated and averaged over multiple cycles. To evaluate stiffness markers (E_P, β, PWV.), average distension, lumen diameter along pressure information is combined.

IV. Results and Discussions

A. Subject Demography

The recruited study group had thirty-four subjects (18 Male and 16 Female) aged 45±17 years with an average systolic blood pressure (SBP) of 137.97±24.05 mmHg and diastolic blood pressure (DBP) of 76.75±12.33 mmHg. Three subjects had a history of smoking, and five subjects had an active lifestyle. Eleven subjects were classified as hypertensive (SBP > 140 mmHg and DBP > 100 mmHg) and twenty-eight as normotensive (SBP: 90 – 140 mmHg, SBP: 60 – 100 mmHg). A summary is shown in TABLE II.

B. Measurement Reliability

The RF signals were reliably captured with an SNR greater than 20 dB, which was sufficient to yield high fidelity diameter waveforms. The diameter waveforms from the left carotid artery obtained after the real-time processing of RF echoes were quasi-periodic and continuous, representing distension of the walls. The average end-diastolic diameter is 5.43±1.52 mm, and distension was 0.55±0.21 mm. A sample of diameter waveform cycles representing different standard morphologies [15], is illustrated in Fig 2. The system could reliably capture these distinct pulse-wave morphologies – Type-A, Type-B and Type-C for respective subjects, allowing reliable model fitting.

The modelling produced distinguishable Gaussian characteristics for the respective morphology categories. It was observed that for Type-A (subjects whose peak systolic pressure occurred after the shoulder point and AIx > 12%) and Type-B (subjects whose peak systolic pressure occurred after the shoulder point, but 0 < AIx < 12%) pulse waves, the ratio of model parameters A_2 and A_1 was greater than 1. Likewise, for Type-C (subjects whose peak systolic pressure preceded a shoulder and AIx < 0), this ratio A_2/A_1 was smaller than 1. In total, 28 subjects were of Type-A or Type-B, and six were of Type-C in this present study group. According to [15], Type-A or Type-B typically represents an older vascular age, and Type-C generally means a younger vascular age. Irrespective of the type of diameter waveform, the sum of the Gaussian model adapts to various types of morphologies for all the subjects, and fitting parameters (A_i, M_i, C_i) and curve fit were successfully obtained the error tolerance, and maximum function calls set for the optimising algorithm.

The τ_R^{GM} was reliably calculated for all subjects and was found to be 54.42±10.33 ms. The range of these measures concurs with earlier reported onset time measures of the early reflections [14]. The diameter waveforms for this study were acquired at 40 Hz, and these were sufficient for the reliable identification of the early reflections' onset time and for the estimation of τ_R^{GM}. Therefore contrary to the methods reported earlier in the literature that requires high-frame-rate or sampling rate acquisition systems [14], the presented method requires low sampling rate diameter signals acquired from an image-free ultrasound system. The ARTSENS system comes with inherent advantages of portability, scalability, operator independence, and affordability [12]. Therefore, it offers a potential and easy to use solution for large scale stiffness-related field studies.

C. Statistical Analysis

The comparison of measurements, τ_R^{GM} versus clinically relevant stiffness markers and versus age were performed based on linear-regression analysis. The correlation strength was shown using the r value and statistical significance through p value ($p < 0.0001$). All average measurements are reported as mean value ± standard deviation.

D. Correlation with Stiffness Markers

Regression plots between the τ_R^{GM}, and clinically relevant stiffness markers are shown in Fig. 3(a) – (c). A statistically significant and strong correlation ($r > 0.849$, $p < 0.0001$) was obtained between τ_R^{GM} and stiffness measures. There exists an inverse correlation between the τ_R^{GM} and all the stiffness markers considered for the study (E_P, β, and PWV). The decreasing trend of the τ_R^{GM} is increasing stiffness values is physiologically rational.

At the macro level, the arterial pulse wave is a combined version of a forward wave with many reflection waves that returns from various branching and peripheral sites in the circulation tree. The distensibility of elastic arteries like aorta, carotid helps in absorbing the pulsatile energy from intermittent ventricular ejection and from reflections sites to maintain steady flow at microcirculation for efficient tissue perfusion. As the artery gets stiffer, there is a loss in the energy storage capacity of the arteries. This increases pulse pressure and pulse wave velocity causing early onset of reflections [4], [16]. Theoretically, stiffer the artery, higher the pulse propagation speed and earlier the onset of reflections. Hence, the onset time of early reflections as captured by the τ_R^{GM} manifested a strong inverse correlation with stiffness markers. This also demonstrated the significance of τ_R^{GM} to be a potential surrogate for arterial stiffness. The advantage being the same can be obtained from any single pulse waveform like diameter.

E. Correlation with Age

A moderate correlation ($r = 0.566$, $p < 0.0001$) was observed between the τ_R^{GM} and age. The relationship has an inverse trend, which again is physiologically explainable. In general, there exists a stiffness gradient from the aorta to peripheral arteries. As age increases, there is a loss in stiffness gradient, that is, the stiffness of central arteries increases to a value closer to the stiffness of peripheral arteries with age[17], [18]. Therefore, the impedance mismatch point between the central and peripheral arteries shifts towards central vessels. This causes reflections to appear early and causes an increase in pulse pressure and PWV. As the reflections appear early with ageing, τ_R^{GM} was able to capture this trend for the recruited subjects successfully.

Although τ_R^{GM} showed statistically significant correlation with age; however, the correlation was lower than that with the stiffness markers. This could be explained by the fact that a person's vascular age need not be the same as the biological age, that is, a young person may have a stiffer artery, therefore, τ_R^{GM} will have a stronger correlation with stiffness than age. Nevertheless, a general trend of stiffer arteries in the older population was observed.

V. Conclusion

In this work, we have presented a novel approach for detecting the onset of early reflections, and hence a surrogate

for arterial stiffness. Arterial diameter waveform was modelled as the sum of three Gaussian curves, and the τ_R^{GM} derived from model parameters obtained by optimisation had statistically significant correlations with age and stiffness markers. The same has been validated in thirty-four subjects. The evidence of the onset of early reflection in the systolic half was reported in the literature for studies that employed a high frame rate – higher bandwidth ultrasound acquisition system. This approach's significance is that only low frame rate diameter waveforms are essential to detect the onset of early reflection waves. Furthermore, this stiffness surrogate is measurable by the proposed method employing diameter waveform alone.

REFERENCES

[1] S. Laurent et al., "Expert consensus document on arterial stiffness: Methodological issues and clinical applications," Eur. Heart J., vol. 27, no. 21, pp. 2588–2605, 2006.

[2] A. P. G. Hoeks, J. M. Willigers, and R. S. Reneman, "Effects of assessment and processing techniques on the shape of arterial pressure-distension loops," J. Vasc. Res., vol. 37, no. 6, pp. 494–500, 2000.

[3] P. M. Nabeel, J. Joseph, S. Karthik, M. Sivaprakasam, and M. Chenniappan, "Bi-Modal arterial compliance probe for calibration-free cuffless blood pressure estimation," IEEE Trans. Biomed. Eng., vol. 65, no. 11, pp. 2392–2404, 2018.

[4] A. Avolio, "Arterial stiffness," Pulse, vol. 1, no. 1, pp. 14–28, 2013.

[5] J. J. Van Der Heijden-Spek, J. A. Staessen, R. H. Fagard, A. P. Hoeks, H. A. Struijker Boudier, and L. M. Van Bortel, "Effect of age on brachial artery wall properties differs from the aorta and is gender dependent: A population study," Hypertension, vol. 35, no. 2, pp. 637–642, 2000.

[6] Y. C. Chiu, P. W. Arand, S. G. Shroff, T. Feldman, and J. D. Carroll, "Determination of pulse wave velocities with computerized algorithms," Am. Heart J., vol. 121, no. 5, pp. 1460–1470, 1991.

[7] P. M. Nabeel, J. Jayaraj, and S. Mohanasankar, "Single source PPG-based local pulse wave velocity measurement: a potential cuffless blood pressure estimation technique," Physiol. Meas., 2017.

[8] P. M. Nabeel, J. Joseph, and M. Sivaprakasam, "A Magnetic Plethysmograph Probe for Local Pulse Wave Velocity Measurement," IEEE Trans. Biomed. Circuits Syst., vol. 11, no. 5, pp. 1065–1076, 2017.

[9] V. K. Raj, P. M. Nabeel, J. Joseph, and M. Sivaprakasam, "Methodological and measurement concerns of local pulse wave velocity assessment," IEEE Int. Symp. Med. Meas. Appl., pp. 1–6, 2019.

[10] P. M. Nabeel, V. K. Raj, J. Joseph, V. V. Abhidev, and M. Sivaprakasam, "Local Pulse Wave Velocity: Theory, Methods, Advancements, and Clinical Applications," IEEE Rev. Biomed. Eng., vol. PP, no. c, pp. 1–1, 2019.

[11] P. Segers et al., "Assessment of pressure wave reflection: Getting the timing right!," Physiol. Meas., vol. 28, no. 9, pp. 1045–1056, 2007.

[12] J. Joseph, P. M. Nabeel, S. R. Rao, R. Venkatachalam, M. I. Shah, and P. Kaur, "Assessment of Carotid Arterial Stiffness in Community Settings with ARTSENS®," IEEE J. Transl. Eng. Heal. Med., vol. 9, no. November 2020, 2021.

[13] C. Liu, D. Zheng, A. Murray, and C. Liu, "Modeling carotid and radial artery pulse pressure waveforms by curve fitting with Gaussian functions," Biomed. Signal Process. Control, vol. 8, no. 5, pp. 449–454, 2013.

[14] E. Hermeling, K. D. Reesink, R. S. Reneman, and A. P. G. Hoeks, "Confluence of incident and reflected waves interferes with systolic foot detection of the carotid artery distension waveform," J. Hypertens., vol. 26, no. 12, pp. 2374–2380, 2008.

[15] J. P. Murgo, N. Westerhof, J. P. Giolma, and S. A. Altobelli, "Aortic Input Impedance in Normal Man: Relationship to Pressure Wave Forms," Circ. J., vol. 62, no. 1, pp. 105–116, 1980.

[16] B. Pannier, A. P. Guérin, S. J. Marchais, M. E. Safar, and G. M. London, "Stiffness of capacitive and conduit arteries: Prognostic significance for end-stage renal disease patients," Hypertension, vol. 45, no. 4, pp. 592–596, 2005.

[17] G. F. Mitchell et al., "Changes in arterial stiffness and wave reflection with advancing age in healthy men and women: The Framingham Heart Study," Hypertension, vol. 43, no. 6, pp. 1239–1245, 2004.

[18] C. Fortier and M. Agharazii, "Arterial Stiffness Gradient," Pulse, vol. 3, no. 3–4, pp. 159–166, 2015.